Inorg. Chem. **2007**, *46*, 3089–3096

Synthesis, Structure, and Magnetic Properties of (A)[Fe^{III}(oxalate)Cl_2] (A = Alkyl Ammonium Cations) with Anionic 1D [Fe^{III}(oxalate)Cl_2]$^-$ Chains

Hong-Bin Xu, Zhe-Ming Wang, Tao Liu, and Song Gao*

Beijing National Laboratory for Molecular Sciences, State Key Laboratory of Rare Earth Materials Chemistry and Applications, College of Chemistry and Molecular Engineering, Peking University, Beijing 100871, P. R. China

Received October 1, 2006

The use of alkyl ammonium cations resulted in four compounds of (A)[Fe^{III}(ox)Cl_2] (A = Et_3NH^+ (**1a**, **1b**), Me_4N^+ (**2**), and *n*-Bu_4N^+ (**3**); ox = oxalate), whose structures and magnetic properties were characterized. In all cases, the metal Fe(III) ions are six-coordinated by four oxygen atoms from two bischelating oxalate ligands and the two terminal Cl^- ions in the cis position. Thus they form similar anionic 1D [Fe^{III}(ox)Cl_2]$^-$ chains. The chains are separated by alkyl ammonium cations in the lattice, and the cation size seems to control the interchain separation and packing patterns in the solid. A parallel arrangement of the [Fe^{III}(ox)Cl_2]$^-$ chains is observed for **1a**, **2**, and **3**, while a crossed one is observed for **1b**, which is a polymorph of **1a**. Magnetic studies reveal the antiferromagnetic intrachain interactions in all compounds. The last three compounds, **1b**, **2**, and **3,** show spin canting below 14.5, 9.5, and 3.8 K, respectively. The dipolar interaction over the interchain distance is proposed to be the result of 3D magnetic ordering in the materials.

Introduction

In the search for new molecule-based magnets during the past decades, oxalato-bridged complexes have been intensively studied because the oxalate (ox) ligands, which adopt bis-bidentate coordination modes, show the ability to mediate magnetic coupling between paramagnetic metal centers separated by more than 5 Å.[1] Many oxalate-bridged dinulcear complexes have been characterized,[2] and the magnetostructural properties have been investigated experimentally[3] and theoretically.[4] It has allowed the rational design of homometallic or heterometallic two-dimensional (2D) and three-dimensional (3D) magnetic networks from a combination of tris(oxalate)metalates [$M^{III}(ox)_3$]$^{3-}$ with other metallic ion precursors using different template cations. This has led to ferro-, (canted) antiferro-, or ferrimagnetic ordering, dependent on the nature of the connected metal ions. At the same time, the introduction of counterions with specific properties could result in polyfunctional materials, with functions such as electrical conductivity,[5] predesigned chirality,[6,7] and nonlinear optical activity.[8]

Recently, intense research efforts have been devoted to the investigation of metal complexes with one-dimensional structures, mainly, because they are suitable examples for

* To whom correspondence should be addressed. Email: gaosong@pku.edu.cn.

(1) For some reviews, see: (a) Kahn, O. *Molecular Magnetism*; VCH: New York, 1993. (b) Rao, C. N. R.; Natarajan, S.; Vaidhyanathan, R. *Angew. Chem., Int. Ed.* **2004**, *43*, 1466. (c) Pilkington, M.; Decurtins, S. *Magnetism: Molecules to Materials II*; VCH: New York, 2002; p 339. (d) Clément, R.; Decurtins, S.; Gruselle, M.; Train, C. *Monatsh. Chem.* **2003**, *134*, 117. (e) Janiak, C. *J. Chem. Soc., Dalton Trans*. **2003**, 2781.

(2) (a) Felthouse, T. R.; Laskowski, E. J.; Hendrickson, D. N. *Inorg. Chem.* **1977**, *16*, 1077. (b) Julve, M.; Verdaguer, M.; Kahn, O.; Gleizes, A.; Philoche-Levisalles, O. *Inorg. Chem.* **1983**, *22*, 368. (c) Julve, M.; Faus, J.; Verdaguer, M.; Gleizes, A. *J. Am. Chem. Soc.* **1984**, *106*, 8306. (d) Castro, I.; Faus, J.; Julve, M.; Mollar, M.; Monge, A.; Gutiérrez-Puebla, E. *Inorg. Chim. Acta* **1989**, *161*, 97. (e) Castro, I.; Faus, J.; Julve, M.; Gleizes, A. *J. Chem. Soc., Dalton Trans.* **1991**, 1937. (f) Soto-Tuero, L.; García-Lozano, J.; Escriva-Monto, E.; Beneto-Borja, M.; Dahan, F.; Tuchagues, J.; Legros, J. P. *J. Chem. Soc., Dalton Trans.* **1991**, 2619. (g) Gleizes, A.; Julve, M.; Verdaguer, M.; Real, J. A.; Faus, J.; Solans, X. *J. Chem. Soc., Dalton Trans.* **1992**, 3209. (h) Vicente, R.; Escuer, Ferretjans, J.; Stoeckli-Evans, H.; Solans, X.; Font-Bardía, M. *J. Chem. Soc., Dalton Trans.* **1997**, 167. (i) Castro, I.; Calatayud, L.; Sletten, J.; Lloret, F.; Julve, M. *J. Chem. Soc., Dalton Trans.* **1997**, 811. (j) Smekal, Z.; Thornton, P.; Sindelar, Z.; Klicka, R. *Polyhedron* **1998**, *17*, 10. (k) Castillo, O.; Muga, I.; Luque, A.; Gutiérrez-Zorrilla, J. M.; Sertucha, J.; Vitoria, P.; Román, P. *Polyhedron* **1999**, *18*, 1237.

(3) (a) Julve, M.; Verdaguer, M.; Kahn, O.; Gleizes, A.; Philoche-Levisalles, O. *Inorg. Chem.* **1984**, *23*, 3808. (b) Glerup, J.; Goodson, P. A.; Hodgson, D. J.; Michelsen, K. *Inorg. Chem.* **1995**, *34*, 6255.

(4) (a) Hay, P. J.; Thibeault, J. C.; Hoffmann, R. *J. Am. Chem. Soc.* **1975**, *97*, 4884. (b) Alvarez, S.; Julve, M.; Verdaguer, M. *Inorg. Chem.* **1990**, *29*, 4500. (c) Escuer, A.; Vicente, R.; Ribas, J.; Jaud, J.; Raynaud, B. *Inorg. Chim. Acta* **1994**, *216*, 139. (d) Román, P.; Guzmán-Miralles, C.; Luque, A.; Beitia, J. I.; Cano, J.; Loret, F.; Julve, M.; Alvarez, S. *Inorg. Chem.* **1996**, *35*, 3741. (e) Cano, J.; Alemany, P.; Alvarez, S.; Verdaguer, M.; Ruiz, E. *Chem.—Eur. J.* **1998**, *4*, 476.

10.1021/ic0618854 CCC: $37.00
Published on Web 03/13/2007

Table 1. Single-Crystal Data and Structure Refinement Details for Compounds **1**−**3**

	1a	1b	2	3
formula	$C_8H_{16}Cl_2FeNO_4$	$C_8H_{16}Cl_2FeNO_4$	$C_6H_{12}Cl_2FeNO_4$	$C_{18}H_{36}Cl_2FeNO_4$
M_r	316.97	316.97	288.92	457.23
cryst syst	triclinic	orthorhombic	monoclinic	monoclinic
space group	$P\bar{1}$	*Fdd*2	$P2_1/c$	$P2_1/c$
a (Å)	10.9609(3)	13.5878(3)	7.9441(3)	8.8836(4)
b (Å)	14.4602(4)	37.9720(10)	8.6093(3)	15.1939(8)
c (Å)	14.5780(4)	10.8210(2)	17.8251(7)	17.9685(12)
α (deg)	85.006(2)	90	90	90
β (deg)	78.845(2)	90	91.869(2)	91.56(3)
γ (deg)	83.0191(12)	90	90	90
V (Å^3)	2245.31(11)	5583.2(2)	1218.47(8)	2424.4(8)
Z	6	16	4	4
ρ_{calcd} (g cm^{-3})	1.406	1.508	1.575	1.253
μ(Mo Kα) (mm^{-1})	1.361	1.461	1.665	0.862
measured reflns	15 299	23 947	21 561	33 390
independent reflns	7904	3186	2798	4223
observed reflns[a]	2925	2060	1580	1254
F(000)	978	2608	588	972
GOF	0.885	0.986	0.902	0.811
max/min (e Å^{-3})	0.802/−0.365	0.667/−0.317	0.344/−0.270	0.338/−0.242
T_{max}/T_{min}	0.856/0.790	0.824/0.705	0.785/0.706	0.990/0.842
R1[b]	0.0672	0.0403	0.0340	0.0613
wR2[c]	0.2125	0.0890	0.0689	0.1024

[a] Observation criterion: $I > 2\sigma(I)$. [b] $R1 = \sum||F_o| - |F_c||/\sum|F_o|$; $I > 2\sigma(I)$. [c] $wR2=\{\sum[w(F_o^2 - F_c^2)^2]/\sum[w(F_o^2)^2]\}^{1/2}$.

the development of models to understand the fundamental factors governing the interactions in extended lattices.[1a,9−11] Some works on neutral homometallic[12−17] and heterometallic[18] one-dimensional chains bridged by the oxalate ion have been reported. As far as we know, few examples have been demonstrated for anionic one-dimensional oxalate-bridged structures with magnetostructural studies.[19,20] For the iron^{III}−oxalate system, only some magnetostructural studies concerning either neutral[21] or anionic[22] dinuclear compounds and two anionic 1D compounds have been known,[20] and recently, a series of three-dimensional Fe-ox and Cl^- compounds was found to show spin-canting magnetic ordering at T_c values ranging from 40 to 70 K,[23] in which the counterions were alkyl ammonium cations, such as NH_4^+, $MeNH_3^+$, $Me_2NH_2^+$, or $EtNH_3^+$. Herein, we report four

(5) (a) Kurmoo, M.; Graham, A. W.; Day, P.; Coles, S. J.; Hursthouse, M.; Caulfield, J. L.; Singleton, J.; Pratt, F. L.; Hayes, W.; Ducasse, L.; Guionneau, P. *J. Am. Chem. Soc.* **1995**, *117*, 12209. (b) Coronado, E.; Galán-Mascarós, J. R.; Gómez-García, C. J.; Laukhin, V. *Nature* **2000**, *408*, 447.

(6) (a) Andrés, R.; Gruselle, M.; Malézieux, B.; Verdaguer, M.; Vaissermann, J. *Inorg. Chem.* **1999**, *38*, 4637. (b) Malézieux, B.; Andrés, R.; Brissard, M.; Gruselle, M.; Train, C.; Herson, P.; Troitskaya, L. L.; Sokolov, V. I.; Ovseenko, S. T.; Demeschik, T. V.; Ovanesyan, N. S.; Mamed'yarova, I. A. *J. Organomet. Chem.* **2001**, *637*−*639*, 182.

(7) (a) Andrés, R.; Brissard, M.; Gruselle, M.; Train, C.; Vaisserman, J.; Malézieux, B.; Jamet, J. P.; Verdaguer, M. *Inorg. Chem.* **2001**, *40*, 4633. (b) Gruselle, M.; Andrés, R.; Malézieux, B.; Brissard, M.; Train, C.; Verdaguer, M. *Chirality* **2001**, *13*, 712.

(8) (a) Bénard, S.; Yu, P.; Audiére, J. P.; Riviére, E.; Clément, R.; Guilhem, J.; Tchertanov, L.; Nakatani, K. *J. Am. Chem. Soc.* **2000**, *122*, 9444. (b) Evans, J. S. O.; Bénard, S.; Yu, P.; Clément, R. *Chem. Mater.* **2001**, *13*, 3813.

(9) *Extended Linear Chain Compounds;* Miller, J. S., Ed.; Plenum: New York, 1983.

(10) *Magnetic Molecular Materials*; Gatteschi, D., Kahn, O., Miller, J. S., Palacio., F., Eds.; D. Reidel: Dordrecht, The Netherlands, 1991; p 198.

(11) *Magneto-Structural Correlation in Exchange-Coupled Systems;* Willet, R. D., Gatteschi, D., Kahn, O., Eds.; D. Reidel: Dordrecht, The Netherlands, 1985.

(12) (a) Castillo, O.; Luque, A.; Román, P.; Lloret, F.; Julve, M. *Inorg. Chem.* **2001**, *40*, 5526. (b) Castillo, O.; Luque, A.; Julve, M.; Lloret, F.; Román, P. *Inorg. Chim. Acta* **2001**, *315*, 9. (c) Castillo, O.; Luque, A.; Lloret, F.; Román, P. *Inorg. Chim. Acta* **2001**, *324*, 141. (d) García-Terán, J. P.; Castillo, O.; Luque, A.; García-Couceiro, U.; Román, P.; Lloret, F. *Inorg. Chem.* **2004**, *43*, 5761. (e) Castillo, O.; Luque, A.; Sertucha, J.; Román, P.; Lloret, F. *Inorg. Chem.* **2000**, *39*, 6142. (f) Castillo, O.; Luque, A.; Iglesias, S.; Guzmán-Miralles, C.; Román, P. *Inorg. Chem. Commun.* **2001**, *4*, 640. (g) Castillo, O.; Luque, A.; Lloret, F.; Román, P. *Inorg. Chem. Commun.* **2001**, *4*, 350. (h) García-Couceiro, U.; Castillo, O.; Luque, A.; García-Terán, J. P.; Beobide, G.; Román, P. *Eur. J. Inorg. Chem.* **2005**, 4280. (i) García-Couceiro, U.; Castillo, O.; Luque, A.; Beobide, G.; Román, P. *Inorg. Chim. Acta* **2004**, *357*, 339. (j) García-Couceiro, U.; Olea, D.; Castillo, O.; Luque, A.; Román, P.; Pablo, P. J.; Gómez-Herrero, J.; Zamora, F. *Inorg. Chem.* **2005**, *44*, 8343.

(13) Li, L.-L.; Lin, K.-J.; Ho, C.-J.; Sun, C.-P.; Yang, H.-D. *Chem. Commun.* **2006**, 1286.

(14) Hursthouse, M. B.; Light, M. E.; Price, D. J. *Angew. Chem., Int. Ed.* **2004**, *43*, 472.

(15) Lethbridge, Z. A. D.; Congreve, A. F.; Esslemont, E.; Slawin, A. M. Z.; Lightfoot, P. *J. Solid State Chem.* **2003**, *172*, 212.

(16) Lu, J. Y.; Schroeder, T. J.; Babb, A. M.; Olmstead, M. *Polyhedron* **2001**, *20*, 2445.

(17) Kim, J. C.; Cho, J.; Lough, A. J. *Inorg. Chim. Acta* **2001**, *317*, 252.

(18) (a) Rochon, F. D.; Robert, M.; Marius, A. *Inorg. Chem.* **1996**, *35*, 6086. (b) Marinescu, G.; Andruh, M.; Lescouëzec, R.; Muñoz, M. C.; Cano, J.; Lloret, F.; Julve, M. *New J. Chem.* **2000**, *24*, 527.

(19) (a) Salta, J.; O'Connor, C. J.; Li, S.-C.; Zubieta, J. *Inorg. Chim. Acta* **1996**, *250*, 303. (b) Coronado, E.; Galán-Mascarós, J. R.; Gómez-García, C. J.; Marti-Gastaldo, C. *Inorg. Chem.* **2005**, *44*, 6197.

(20) (a) Zhang, B.; Wang, Z. -M.; Fujiwara, H.; Kabayashi, H.; Kurmoo, M.; Inoue, K.; Mori, T.; Gao, S.; Zhang, Y.; Zhu, D. B. *Adv. Mater.* **2005**, *17*, 1988. (b) Zhang, B.; Wang, Z. M.; Zhang, Y.; Takahashi, K.; Okano, Y.; Cui, H.-B.; Kabayashi, H.; Kurmoo, M.; Inoue, K.; Kurmoo, M.; Pratt, F. L.; Zhu, D. B. *Inorg. Chem.* **2006**, *45*, 3275.

(21) Julve, M.; Kahn, O. *Inorg. Chim. Acta.* **1983**, *76*, L39.

(22) (a) Coronado, E.; Galán-Mascarós, J. R.; Gómez-García, C. J. *J. Chem. Soc., Dalton Trans.* **2000**, 205. (b) Rashid, S.; Turner, S.; Day, P.; Light, M. E.; Hursthouse, M. B. *Inorg. Chem.* **2000**, *39*, 2426. (c) Triki, S.; Bérézovsky, F.; Sala Pala, J.; Coronado, E.; Gómez-García, C. J.; Clemente, J. M.; Riou, A.; Molinié, P. *Inorg. Chem.* **2000**, *39*, 3771. (d) Armentano, D.; De Munno, G.; Faus, J.; Lloret, F.; Julve, M. *Inorg. Chem.* **2001**, *40*, 655.

(23) (a) Armentano, D.; Munno, G. D.; Lloret, F.; Palii, A. V.; Julve, M. *Inorg. Chem.* **2002**, *41*, 2007. (b) Armentano, D.; Munno, G. D.; Mastropietro, T. F.; Julve, M.; Lloret, F. *Chem. Commun.*, **2004**, 1160. (c) Armentano, D.; Munno, G. D.; Mastropietro, T. F.; Proserpio, D. M.; Julve, M.; Lloret, F. *Inorg. Chem.* **2004**, *43*, 5177. (d) Armentano, D.; Munno, G. D.; Mastropietro, T. F.; Julve, M.; Lloret, F. *J. Am. Chem. Soc.* **2005**, *127*, 10778.

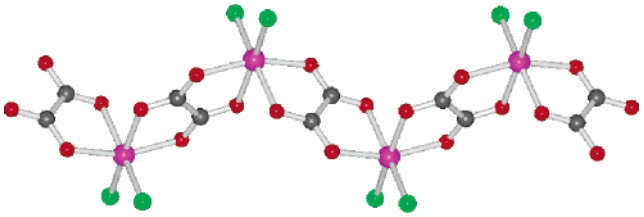

Figure 1. Representative view of a fragment of the anionic chain. Color scheme: C, gray; O, red; Cl, green; Fe, purple.

anionic one-dimensional $[Fe^{III}(ox)Cl_2]^-$ chain structures, {-(A)$[Fe^{III}(ox)Cl_2]$} (A = Et_3NH^+, **1a**, **1b**; Me_4N^+, **2**; *n*-Bu_4N^+, **3**) using other larger alkyl ammonium cations as counterions. These chains exhibit moderate antiferromagnetic intrachain coupling between iron(III) atoms bridged by oxalato ligands. Spin-canting antiferromagnetic ordering was observed in compounds **1b**, **2**, and **3** with different T_c values of 14.5, 9.5, and 3.8 K, corresponding to the different arrangements and the separation of the chains. Long-range magnetic ordering might come from the contribution of the dipolar interaction between the chains separated by cations over the large distance.

Experimental Section

Synthesis. All starting materials were commercially available, reagent grade, and used without further purification.

(Et_3NH)[Fe^{III}(ox)Cl$_2$], 1a. $FeCl_3 \cdot 6H_2O$ (1.0 mmol) and oxalic acid (1.0 mmol) were dissolved in 10 mL of water, and triethylamine (0.30 mL, 2.2 mmol) was added. Brick red precipitates were formed. After 2 h, it was filtered, and the filtrate was left undisturbed at room temperature. Slow evaporation of the solution gave dark-green needle crystals of **1a** and yellow-green block crystals of **1b** in one week (yield = 30%). Pure **1a** was separated manually for all measurements. Anal. (%) Calcd for $C_8H_{16}NO_4Cl_2Fe$: C, 30.31; N, 4.42; H, 5.09. Found: C, 30.92; N, 4.79; H, 5.51. IR (cm^{-1}): ν 3136w, 2987w, 2803w, 1692s, 1609s, 1457w, 1400w, 1349w, 1306w, 806m.

(Et_3NH)[Fe^{III}(ox)Cl$_2$], 1b. The synthesis of **1b** was similar to that of **1a** except that the amount of triethylamine used was 0.20 mL (1.4 mmol). Some brick red precipitates were formed immediately and then dissolved by stirring. Yellow green block crystals were obtained in an 80% yield. Anal. (%) Calcd for $C_8H_{16}NO_4Cl_2Fe$: C, 30.31; N, 4.42; H, 5.09. Found: C, 29.96; N, 4.24; H, 5.09. IR (cm^{-1}): ν 3137w, 2984w, 2948w, 1697m, 1608s, 1472w, 1399w, 1349w, 1307w, 805m.

(Me_4N)[Fe^{III}(ox)Cl$_2$], 2. The synthesis of **2** was similar to that of **1a**, but tetramethyl ammonium hydroxide (1.2 mL 10% aqueous solution) was used instead of triethylamine. Bright green needle crystals were harvested in a 70% yield. Anal. (%) Calcd for $C_6H_{12}NO_4Cl_2Fe$: C, 24.94; N, 4.85; H, 4.19. Found: C, 24.52; N, 5.03; H, 4.40. IR (cm^{-1}): ν 3398w, 3054w, 2972w, 1695s, 1606s, 1484s, 1350w, 1308w, 946w, 805m.

(*n*-Bu_4N)[Fe^{III}(ox)Cl$_2$], 3. The synthesis of **3** was similar to that of **1a**, but tetrabutyl ammonium hydroxide (2 mL 10% aqueous solution) was used instead of triethylamine. The products are yellow needle crystals (yield 60%). Anal. (%) Calcd for $C_{18}H_{36}NO_4Cl_2Fe$: C, 47.28; N, 3.06; H, 7.94. Found: C, 47.02; N, 2.95; H, 7.88. IR (cm^{-1}): ν 2959w, 2974w, 1691s, 1605s, 1490s, 1381w, 1350w, 1308w, 886w, 804m.

X-ray Crystallography. Crystallographic data for single crystals of all compounds were collected[25] at room temperature on a Nonius KappaCCD diffractometer with a 2.0 kW sealed-tube source using graphite-monochromated Mo Kα radiation of λ = 0.71073 Å. Empirical absorption corrections were applied using the Sortav program.[26] The structures were solved by direct methods and were refined with the full-matrix least-squares method on F^2 with anisotropic thermal parameters for all non-hydrogen atoms. The hydrogen atoms of cations were added by calculated positions. Some constraints were applied for disordered cations. All structure calculations were performed using the SHELX program.[27] Crystallographic data are listed in Table 1. Selected molecular and hydrogen bonding geometries are given in Tables S1−S4. Powder X-ray diffaraction patterns were obtained on a Rigaku RINT2000 diffractometer at room temperature with Cu Kα radiation in a flat-plate geometry.

Physical Measurements. Elemental analyses of carbon, hydrogen, and nitrogen were carried out with an Elementar Vario EL. The IR spectra were recorded on a Magna-IR 750 spectrophotometer in the 4000−650 cm^{-1} range against pure samples. Magnetic study was performed on a Quantum Design MPMS 5XL SQUID system. Diamagnetic corrections were estimated using Pascal constants[24] (-166×10^{-6} for **1a** and **1b** and -146×10^{-6} and -287×10^{-6} for **2** and **3**, respectively) and background correction by experimental measurement of the sample holders. Thermal gravimetric analysis, TGA, was performed on a SDT 2960 thermal analyzer for **1a** and **1b** at 10 °C min^{-1} under air.

Results and Discussion

Synthesis and IR Spectra. As mentioned above, oxalato-bridged complexes are well-known to construct 0D−3D structures. However, for the iron^{III}−oxalate system, only a few results were reported for 0D, 1D, and 3D complexes.[20−23] Julve and co-workers have reported a series of 3D iron^{III}−oxalate complexes with both oxo and oxalate bridges. Alkyl ammonium cations, NH_4^+, $MeNH_3^+$, $Me_2NH_2^+$, or $EtNH_3^+$, seem to play an important role for the formation of the high-dimensional structures in this family. Our attempt to synthesize Fe^{III}−ox compounds using some larger alkyl ammonium cations, however, afforded another series of similar anionic 1D zigzag $[Fe^{III}(ox)Cl_2]^-$ chains, despite the diverse cations and pH values of the system. The larger alkyl ammonium cations might have less possibility to be accommodated by the 3D Fe^{III}−ox framework but inhibit the formation of higher-dimensional frameworks. The higher pH value in solution could not result in the existence of the oxo bridge. So it seems that the larger counterions in these systems are inclined toward the 1D zigzag structure, which proved the similar 1D chain structures.

Compounds **1a** and **1b** are polymorphs. They were synthesized under different triethylamine concentrations. In our case, the solution of $FeCl_3 \cdot 6H_2O$ and oxalic acid turned

(24) Mulay, L. N.; Boudreaux, E. A. *Theory and Applications of Molecular Diamagnetism*; John Wiley & Sons Inc.: New York, 1976.
(25) (a) *Collect, Data Collection Software*; Nonius B.V.: Delft, The Netherlands, 1998. (b) *HKL2000* and *maXus*; University of Glasgow: Glasgow, Scotland, U.K.; Nonius BV: Delft, The Netherlands; MacScience Co. Ltd.: Yokohama, Japan, 2000.
(26) (a) Blessing, R. H. *Acta Crystallogr.* **1995**, *A51*, 33. (b) Blessing, R. H. *J. Appl. Crystallogr.* **1997**, *30*, 421.
(27) (a) Sheldrick, G. M. *SHELXTL*, version 5.1; Bruker Analytical X-ray Instruments Inc.: Madison, WI, 1998. (b) Sheldrick, G. M. *SHELX-97*, PC version; University of Göttingen: Göttingen, Germany, 1997.

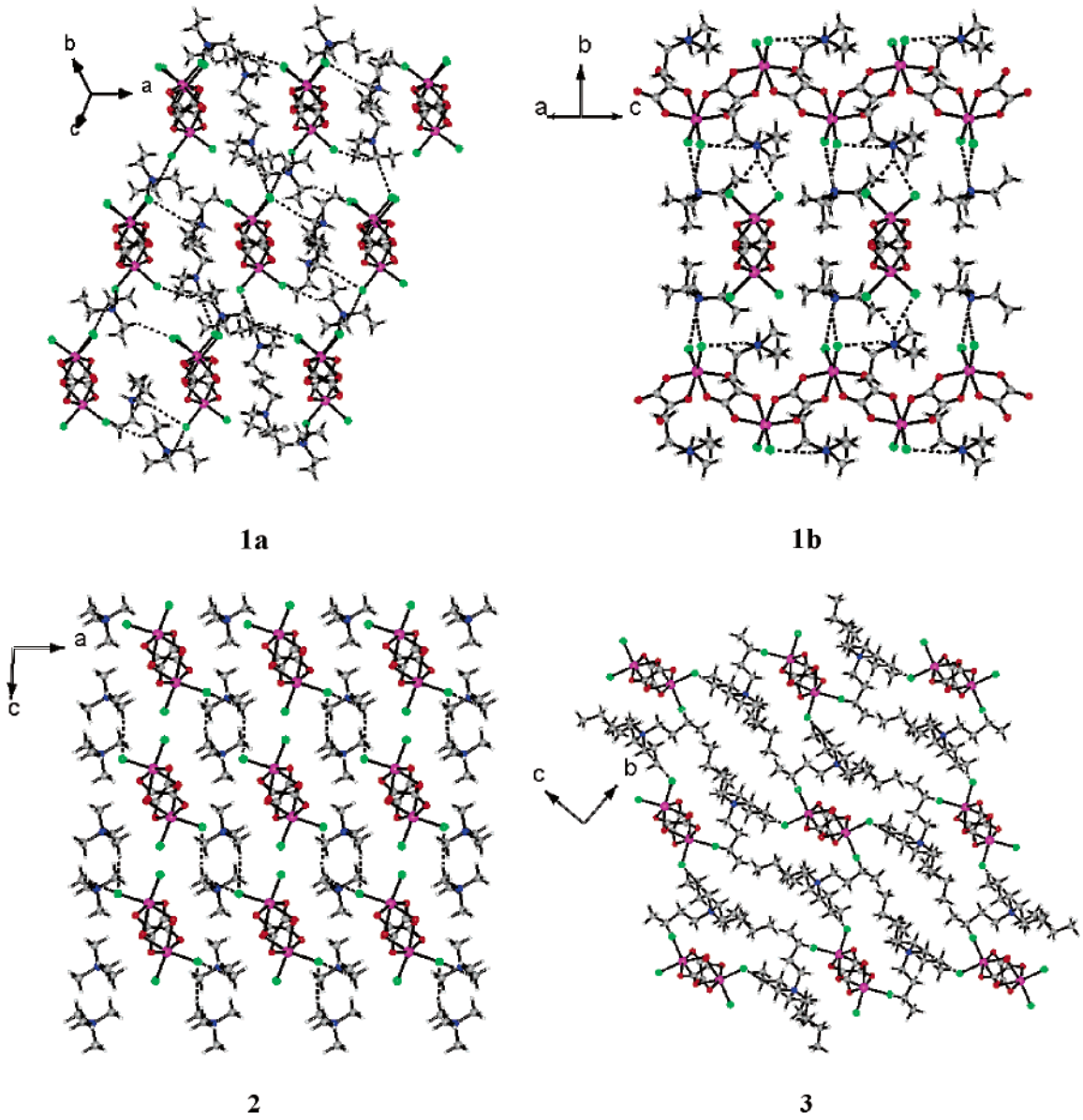

Figure 2. Crystal packing of compounds **1**−**3**. C−H···Cl hydrogen bonds are drawn as dotted lines. Color scheme: C, gray; O, red; N, blue; H, white; Cl, green; Fe, purple.

cloudy after the addition of 0.20 mL of triethylamine, and when 0.30 mL of triethylamine was added, some precipitates were formed and could not be dissolved. More triethylamine only resulted in more precipitates, and we could not get any crystals. However, we got the mixture of **1a** and **1b** in the later solution, and the attempt to obtain **1a** as a single product in one batch was unsuccessful. The pure **1a** sample was isolated manually. Powder X-ray diffraction patterns (Figure S1) confirm the phase purity of all four compounds.

The IR spectra of the four compounds are similar to one another, with characteristic IR bands for protonated amine cations and oxalate groups. Some of the main IR absorptions can be assigned as follows: 3137w−2803w for ν(N−H) and ν_s(C−H), 1697s−1605s for ν_{as}(O−C−O), 1447m−1484m for ν(C−N), 1306w−1350w for ν_s(O−C−O), 804−806 m for δ(O−C−O), which are co-incident with those previously reported values.[12,23,28] The frequencies of the symmetric and antisymmetric carboxylate mode of oxalato ion in the present compounds are not affected by different cations. Therefore, it seems that these local modes depend solely on the local geometry of the O−C−O group and not on its surroundings.

Crystal Structure. Each of the compounds possesses an anionic structure unit composed of a 1D $[Fe^{III}(ox)Cl_2]^-$ zigzag chain (Figure 1), which has been observed in only a few compounds before.[20] In the chain, the Fe^{3+} ions are sequentially bridged by the bis-bidentate oxalate dianion in the cis position and coordinated by two terminal Cl^- ions to complete the distorted octahedral coordinated environment. The Fe−O (2.026−2.200 Å) and Fe−Cl distances (2.224 to 2.352 Å) (Tables S1−S4) are similar to those reported in

(28) Wang, Z.-M.; Zhang, B.; Otsuka, T.; Inoue, K.; Kabayashi, H.; Kurmoo, M. *J. Chem. Soc., Dalton Trans.* **2004**, 2209.

Table 2. Selected Magnetostructural Data for Known Oxalate-Bridged Iron(III) Anionic 1D [Fe^{III}(ox)Cl$_2$]$^-$ Structures[a]

	1a	1b	2	3	4	5
Fe···O$_{ox}$ (Å)	2.035(5)	2.034(3)	2.0260(2)	2.047(4)	2.049(3)	2.034(4)
	2.043(4)	2.038(3)	2.0621(2)	2.061(4)	2.059(3)	2.151(4)
	2.145(5)	2.116(3)	2.1261(2)	2.137(4)	2.059(3)	
	2.200(5)	2.163(3)	2.1624(2)	2.141(4)	2.137(3)	
intrachain	5.457	5.465	5.487	5.490	5.494	5.447
Fe···Fe (Å)	5.470		5.472	5.484		
	5.530					
	5.473					
interchain	8.345	8.276	7.314	10.463	7.383	8.903
Fe···Fe (Å)	8.437	8.433	7.994	15.194	11.012	19.493
	8.978	8.685	9.659	15.362	11.417	23.586
	14.657		11.828			
Fe···Fe···Fe (deg)	104.15	105.24	103.56	108.10	108	102
	101.69					
	109.16					
a (deg)	82.4	77.9	78.3	85.6	89.8	98.7
	77.9					
	77.0					
T_{max} (K)	40	50	48	42	55	50
T_c (K)		14.5	9.5	3.8	19.8	4.5
C (cm^3 K mol^{-1})	4.62	5.03	4.48	4.84	4.83	4.81
θ (K)	−93.9	−112.0	−99.7	−98.0	−21.4	−107
J (cm^{-1})	−3.63	−4.28	−3.97	−3.76	−5.1	
G	1.98	2.06	1.95	2.03	2 (fixed)	

[a] The abbreviations used are as follows. Fe−O$_{ox}$ = iron-oxalate oxygen bond. For compound **1**, only Fe1−O$_{ox}$ values are listed. Fe···Fe···Fe = the angle of the adjacent Fe atoms bridged by ox ligands. α = dihedral angles between the oxalato mean planes. T_{max} = the temperature value according to the maximum magnetic susceptibility in the χ_M vs T plot in high-temperature region. T_c = the bifurcation temperature in ZFC/FC measurements. C = Curie constants. θ = Weiss constants. J = the exchange constant between the iron(III) ions through the bridging oxalate ion. Compounds **4** and **5** refer to TTF[Fe^{III}(ox)Cl$_2$] and κ-BETS$_2$[Fe^{III}(ox)Cl$_2$], respectively, from ref 20.

oxalato-bridged iron(III) complexes in the literature.[21−23] While the countercations of alkyl amine do not change the structure of the anionic [Fe^{III}(ox)Cl$_2$]$^-$ chain much more, they seem to control the arrangement of the chains and the interchain interactions in crystals. The cations provide not only the charge balance but also the hydrogen bond interactions (Tables S1−S4), both conventional and weak, to glue the counterpart of the structure. More structural details concerning the individual compounds, especially the packing patterns and interchain separations (Figure 2) are discussed below.

(Et$_3$NH)[Fe^{III}(ox)Cl$_2$] 1a and **1b.** Compounds **1a** and **1b** are polymorphs, containing the same anionic [Fe^{III}(ox)Cl$_2$]$^-$ chains and Et$_3$NH$^+$ cations while showing different packing arrangement in crystal structure. **1a** crystallizes in the triclinic space group $P\bar{1}$. The asymmetric unit consists of three unique [Fe^{III}(ox)Cl$_2$]$^-$ units and three Et$_3$NH$^+$ cations. The three independent Fe sites have a Λ configuration for Fe1 and Fe3 and Δ for Fe2; however, along the chain, the Fe sites are still arranged in a ΛΔΛΔ sequence because the unique trimeric segments of {[Fe^{III}(ox)Cl$_2$]$_3$}$^{3-}$ are centrosymmetrically related to each other via the ox bridges. Four unique Fe···Fe distances via ox (5.457, 5.470, 5.530, and 5.473 Å) are observed in the chain; the dihedral angles between the adjacent oxalates are 77.4, 77.8, and 82.2°, and the Fe···Fe···Fe angles are 101.69, 104.15, and 109.16°, respectively.

In the lattice (Figure 2a), the [Fe^{III}(ox)Cl$_2$]$^-$ chains run along the body-diagonal direction of [111], and they are arranged roughly in a hexagonal packing. The [Fe^{III}(ox)Cl$_2$]$^-$ chains are surrounded by arrays of countercations. In fact, the cations of Et$_3$NH$^+$ form cationic wavelike layers which isolate the [Fe^{III}(ox)Cl$_2$]$^-$ chains well. Some short interchain Fe···Fe distances are 8.345−8.978 Å.

Compound **1b** belongs to the orthorhombic space group *Fdd*2. Only one unique [Fe^{III}(ox)Cl$_2$]$^-$ unit is in the anionic chain, and the unique Fe···Fe distance via ox, the dihedral angle between ox groups, and the Fe···Fe···Fe angle are 5.465 Å, 77.9°, and 105.2°, respectively. **1b** displays interesting packing in the lattice (Figure 2b), different from that of **1a**. This distinct feature comes from the fact that the [Fe^{III}(ox)Cl$_2$]$^-$ chains run along two different directions, $a + c$ and $a-c$, in the lattice, with an angle of 77° between the two directions. The chains form layers parallel to the *ac* plane; in each layer, the chains run parallel, while those of adjacent layers are crossed, resulting in a staggered packing pattern of [Fe^{III}(ox)Cl$_2$]$^-$ chains in the lattice. This is unusual because in most 1D compounds the chains are usually arranged in a parallel manner. Again, the cations of Et$_3$NH$^+$ form cationic layers to separate layers of anionic chains and have their branches inserted into the interchain region in each anionic layer, thus isolating the [Fe^{III}(ox)Cl$_2$]$^-$ chains. The short interchain Fe···Fe separations are 8.276−8.685 Å. It is worth noting that the higher density and thus smaller volume per (Et$_3$NH)[Fe^{III}(ox)Cl$_2$] of **1b** than that of **1a** (Table 1) indicates that **1b** is probably the more thermodynamically stable phase. TGA has been performed (Figure S2); however, we could not conclude directly which one is more stable (**1a** vs **1b**) because the first weight losses occurred at almost the same temperature region.

(Me$_4$N)[Fe^{III}(ox)Cl$_2$], 2, and (*n*-Bu$_4$N)[Fe^{III}(ox)Cl$_2$], 3. The use of a small cation of Me$_4$N$^+$ and a large one of

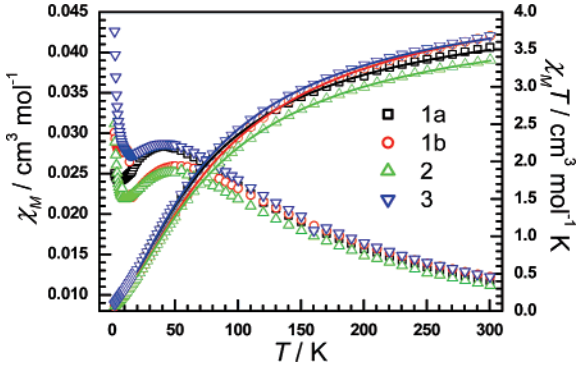

Figure 3. Plot of $\chi_M T$ vs T for **1**−**3** in an applied field of 1 kOe from 2 to 300 K; solid lines represent the best theoretical fit (see text) for the data above 20 K.

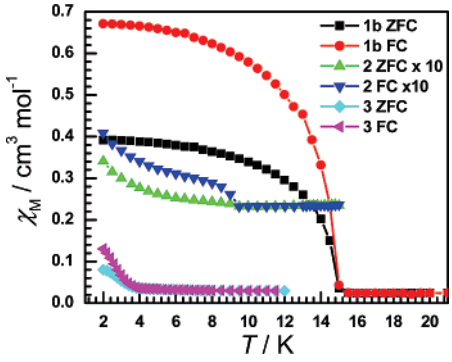

Figure 4. ZFC/FC measurements for compounds **1b**−**3** in an applied field of 20 Oe. The data for compound **2** have been multiplied by 10.

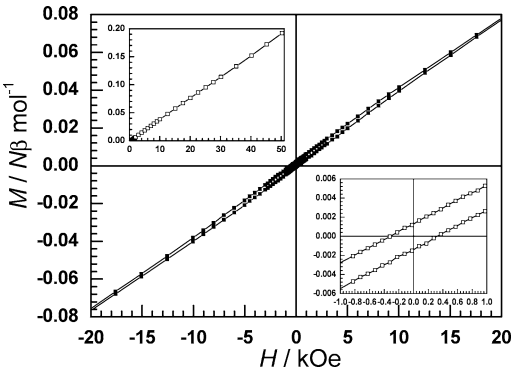

Figure 5. Hysteresis loop measured for **1b** at 1.9 K. Inset: Field dependence of isothermal magnetization $M(T,H)$ for **2** at 2 K from 0 to 50 kOe and the expanded low-field region for clarity.

n-Bu_4N^+ afforded compounds **2** and **3** with the same $[Fe^{III}(ox)Cl_2]^-$ chains. While little change is observed in the structural parameters of the $[Fe^{III}(ox)Cl_2]^-$ chain (Table S3 and S4), the cation size determines the interchain separation in solids. In the lattice of **2** (Figure 2c), the $[Fe^{III}(ox)Cl_2]^-$ chains are arranged in a parallel manner, extending along the *b* direction, with the cations between them. The two short and two long Fe···Fe separations between chains are in the range of 7.314−11.828 Å. While for **3** (Figure 2d), the $[Fe^{III}(ox)Cl_2]^-$ chains, along the *a* direction, are well isolated by the largest cation, n-Bu_4N^+, used in this work, with the shortest interchain Fe···Fe separation of 10.463 Å.

As far as we know, there are only six 1D Fe^{III}−ox chain compounds reported up to now, and the related structural data are listed in Table 2. The distances between the Fe atoms and the oxygen atoms of the ox ion are in the range of 2.026−2.200 Å, and the distances between the adjacent Fe atoms bridged by ox ligands are in 5.447−5.494 Å range, which is similar to those reported in the literature.[29,30] However the angles of the adjacent Fe atoms bridged by ox ligands and dihedral angles between the ox mean planes are extended to 101.69−109.12° and 77.0−98.7°, respectively, on a comparatively large scale, which demonstrates the great flexibility in the geometry of the $[Fe^{III}(ox)Cl_2]^-$ chain to match cations of different sizes and arrangements.

Magnetism. The temperature dependence of the magnetic susceptibility for **1**−**3** in an applied field of 1 kOe shows mainly antiferromagnetic character (Figure 3). In the high-temperature region, the four compounds behave similarly. At room temperature, the $\chi_M T$ values are 3.35−3.68 cm^3 K mol^{-1}. These values continuously decrease, upon cooling, from 300 K to 0.050−0.085 at the lowest temperature of 2 K. The χ_M values display a broad maximum at 40−50 K. The magnetic susceptibilities in the range of 120−300 K obey the Curie−Weiss law with $C = 4.48$−5.03 cm^3 mol^{-1} K, $\theta = -93.9$ to -112 K for the compounds (Table 2). This indicates the presence of the antiferromagnetic coupling between Fe(III) ions. For **1b**, **2**, and **3**, the sharp rise of the χ_M versus T plots in the low temperature is observed, indicating possible weak ferromagnetism, while **1a** shows no evidence of spin canting.

The occurrence of the weak ferromagnetism in **1b**, **2**, and **3** is further characterized by the zero-field-cooled (ZFC) and field-cooled (FC) measurements at low field (Figure 4). The irreversibility is clear below the bifurcation temperatures of 14.5, 9.5, and 3.8 K for **1b**, **2**, and **3**, respectively. The isothermal magnetization plots (Figure 5, Figures S3−S5 in the Supporting Information) at 2 K for all the materials increase almost linearly from 0 to 50 kOe and reach 0.23, 0.19, 0.20, and 0.27 μ_B, respectively, per Fe(III) ion at 50 kOe, far from the saturation values of $M_S = 5\ \mu_B$ for a spin-only Fe(III) ion, confirming the antiferromagnetic coupling between the Fe(III) ions. For **1b**, a hysteresis loop can be observed at 1.9 K with a coercivity field, H_c, of about 350 Oe and a remnant magnetization, M_R, of 0.0028 μ_B. From the remnant magnetization and the expected value of 5 μ_B for spin $S = 5/2$, a small value of the canting angle of about 0.03° is estimated.

Taking into account the 1D chain structure, we fit the experimental data by means of an $S = 5/2$ Fisher chain model ($H = -2J\sum S_i S_{i+1}$)[29] in the 20−300 K range for the four compounds and get best-fit parameters: $J = -3.63$ to -4.28 cm^{-1}, $g = 1.95$−2.06 (Table 2), with R less than 10^{-4}, where R is the agreement factor defined as $R = \sum[(\chi_M T)_{obsd} - (\chi_M T)_{calcd}]^2/\sum[(\chi_M T)_{obsd}]$.[2] The exchange interactions in these compounds are in good agreement with the reported results of neutral[30] and anionic[31] dinuclear compounds and a similar anionic 1D compound[20] (J values range from -3.44 cm^{-1} to -7.22 cm^{-1}).

(29) Kahn, O. *Molecular Magnetism*; VCH: New York, 1993; p 258.
(30) (a) Julve, M.; Kahn, O. *Inorg. Chim. Acta* **1983**, *76*, L39. (b) Lloret, F.; Julve, M.; Faus, J.; Journaux, Y.; Philoche-Levisalles, M.; Jeannin, Y. *Inorg. Chem.* **1989**, *28*, 3702.

In consideration of their magnetic properties, in all compounds, the presence of mediate antiferromagnetic intrachain coupling is observed between Fe(III) ions through the ox bridge (Table 2). The exchange coupling, *J*, in the range from -3.63 cm^{-1} to -5.10 cm^{-1}, demonstrates some distinction of the strength of coupling between these compounds, **4** > **1b** > **2** > **3** >**1a**, which also could be determined from the value of the temperature with the magnetic susceptibility maximum in curve $\chi_M(T)$ and the value of the critical temperature of the compounds in our cases. At the same time, they show weak ferromagnetic ordering at low temperature, except for compound **1a**. There are two mechanisms which lead to spin canting, namely, magnetic anisotropy and antisymmetric exchange. Fe(III) ion is more isotropic, the most likely anisotropy is from second-order spin−orbit coupling, which is usually weak on the geometry. On the other hand, the last three compounds, **1b**, **2**, and **3**, are crystallized in the noncentered and centered symmetric space group, respectively (*Fdd*2 and $P2_1/c$); however the neighboring spin-carrier Fe(III) ions, through the bridging ox ligands in the unit cell, are not related by an inversion center, and the spin-canting in the chain may arise from the canting of the spins caused by the Dzyaloshinsky−Moriya (D−M) interaction.[32] The bulk weak ferromagnetism should be from the cooperative interaction between the canting 1D [Fe^{III}(ox)Cl$_2$]$^-$ chain. From the perspective view of the three-dimensional stack (Figure 2), where superexchange interaction can be neglected because of large interchain spacing, dipole−dipole interactions between the chains and the hydrogen bonds, mediated by ammonium cations, might be responsible for the long-range ordering. Considering the large, flexible, and non-conjugated ammonium ions in these materials, the dipolar interaction would be more important, especially for these high-spin (5/2) iron(III) ions, as proposed by the dipolar interaction mechanism. The dipolar interaction is proportional to R^{-3}, where *R* is the distance between the spin centers. If the moments are large, dipolar interaction could become more important in the molecular magnet at a large distance, and although it might be rather weak, it may be strong enough to induce three-dimensional magnetic ordering in clusters,[33] chains,[34] and layers.[35] From the detailed data of all compounds **1**−**3** (Table 2), the separations of the chains are distinct from each other because of the occupation of the respective ammonium cations between the chains. In compound **1b**, the chains have three closest neighbors (8.276−8.685 Å) and arrange in a staggered mode; thus, **1b** shows highest T_c (14.5 K) in our study. There are two short separations (7.314 and 7.944 Å) and two long ones (9.659 and 11.828 Å) in compound **2,** in which T_c becomes 9.5 K. For compound **3**, four large separations, all above the 10 Å, make the critical temperature as low as 3.8 K. Nevertheless, both of the dipolar and hydrogen-bond interactions are present in compound **4** and **5** as a result of rigid and conjugated radical cations; moreover there might be a π−d interaction between the conduction electrons from the TTF and the d electrons from the metal ions. Therefore, they have a slightly higher T_c temperature in the similar condition. While compound **1a** crystallized in the triclinic system, space group, $P\bar{1}$, for which the weak ferromagnetism is forbidden.[36] Although a few complexes with triclinic systems were reported to show weak ferromagnetism,[37] their structures were not determined at low temperature, and they might have another symmetry when they have cooled down and approached the transition temperature. Compound **1a** might retain crystallographic symmetry to 2 K, and no ordering state was observed. Recently, a neutral, similar zigzag chain structure Fe^{II}−ox−phen was reported[38] with spin-canting at low temperature. However, the central metal is the more anisotropic Fe^{II}, and the compound is crystallized in the chiral spacegroup $P2_1$; furthermore, the ferromagnetic coupling through the π-stacked phen ligands might also contribute to the observed ferromagnetism at low temperature. While in our case, dipolar interaction would be responsible for the long-range ordering through the large separation of the anionic 1D [Fe^{III}(ox)Cl$_2$]$^-$ chains. This kind of anionic 1D [Fe^{III}(ox)Cl$_2$]$^-$ structure could show great flexibility and diverse magnetism, and it might be a good precursor to polyfunctional materials combined with the cationic part with special properties.[20]

Conclusion

The use of different alkyl-substituted ammonium derivatives as counterions has led to the synthesis of a small family of {(A)[Fe^{III}(ox)Cl$_2$]} (A = Et$_3$NH$^+$, **1a**, **1b**; Me$_4$N$^+$, **2**; *n*-Bu$_4$N$^+$, **3**). They have similar anionic 1D [Fe^{III}(ox)Cl$_2$]$^-$ chain structures and have much flexibility to accommodate different cations. Despite the structural similarities, their

(31) (a) Coronado, E.; Galán-Mascarós, J. R.; Gómez-García, C. J. *J. Chem. Soc., Dalton Trans.* **2000**, 205. (b) Rashid, S.; Turner, S.; Day, P.; Light, M. E.; Hursthouse, M. B. *Inorg. Chem.* **2000**, *39*, 2426. (c) Triki, S.; Bérézovsky, F.; Sala Pala, J.; Coronado, E.; Gómez-García, C. J.; Clemente, J. M.; Riou, A.; Molinié, P. *Inorg. Chem.* **2000**, *39*, 3771. (d) Armentano, D.; De Munno, G.; Faus, J.; Lloret, F.; Julve, M. *Inorg. Chem.* **2001**, *40*, 655.

(32) Carlin, R. L.; Van-Duyneveldt, A. J. *Magnetic Properties of Transition Metal Compounds*; Springer-Verlag: New York, 1977.

(33) (a) Morello, A.; Mettes, F. L.; Bakharev, O. N.; Brom, H. B.; Jongh, L. J.; Lu, F.; Fernández, J. F.; Aromí, G. *Phys. Rev. B.* **2006**, *73*, 134406. (b) Affonte, M.; Lasjaunias, J. C.; Wernsdorfer, W.; Sessoli, R.; Gatteschi, D.; Heath, S. L.; Fort, A.; Rettori, A. *Phys. Rev. B.* **2002**, *66*, 064408.

(34) (a) Wynn, C. M.; Gîrtu, M. A.; Brincherhoff, W. B.; Sugiura, K.-I.; Miller, J. S.; Epstein, A. P. *Chem. Mater.* **1997**, *9*, 2156. (b) Ostrovsky, S.; Haase, W.; Drillon, M.; Panissod, P. *Phys. Rev. B.* **2001**, *64*, 134418.

(35) (a) Kurmoo, M. *Chem. Mater.* **1999**, *11*, 3370. (b) Kurmoo, M.; Day, P.; Derory, A.; Estournès, C.; Poinsot, R.; Stead, M. J.; Kepert, C. J. *J. Solid State Chem.* **1999**, *145*, 452. (c) Drillon, M.; Panissod, P. *J. Magn. Magn. Mater.* **1998**, *188*, 93.

(36) Authier A. *International Tables for Crystallography, Volume D, Physical Properties of Crystals*; Kluwer Academic Publishers: Dordrecht, The Netherlands, 2003.

(37) (a) Song, Y.; Zavalij, P. Y.; Chernova, N. A.; Whittingham, M. S. *Chem. Mater.* **2003**, *15*, 4968. (b) Ray, U.; Jasimuddin, S.; Ghosh, B. K.; Monfort, M.; Ribas, J.; Mostafa, G.; Lu, T.-H.; Sinha, C. *Eur. J. Inorg. Chem.* **2004**, 250. (c) Figuerola, A.; Ribas, J.; Casanova, D.; Maestro, M.; Alvarez, S.; Diaz, C. *Inorg. Chem.* **2005**, *44*, 6949. (d) Riou-Cavellec, M.; Lesaint, C.; Noguès, M.; Grenèche, J.; Férey, G. *Inorg. Chem.* **2003**, *42*, 5669. (e) Fernandez, S.; Mesa, J. L.; Pizarro, J. L.; Peña, A.; Chapman, J. P.; Arriortua, M. I. *Mater. Res. Bull.* **2004**, *39*, 1779.

(38) Li, L.-L.; Lin, K.-J.; Ho, C.-J.; Sun, C.-P.; Yang, H.-D. *Chem. Commun*. **2006**, 1286.

magnetic behaviors range from paramagnetic to spin-canting antiferromagnetic (T_c = 3.8−14.5 K). The dipolar interaction will be responsible for this kind of long-range magnetic ordering because of the large space between the chains.

Acknowledgment. We are grateful to Prof. Zhang B for her kind discussion and help. This work is supported by NSFC (20221101, 20490210, 20571005), the National Basic Research Program of China (2006CB601102), and the Research Fund for the Doctoral Program of Higher Education (Grant 20050001002).

Supporting Information Available: X-ray crystallographic files in CIF format and a PDF file containing Tables S1−S4 and Figures S1−S5. This material is available free of charge via the Internet at http://pubs.acs.org.

IC0618854